

Detection of a fault zone in the south of Bam using CSTMT method

Moghadas, D.¹, Oskooi, B.^{2*}, Hashemi Tabatabaei, S.³, Pesersen, L.⁴ and Nasuti, A.⁵

¹ Master Graduate, Institute of Geophysics, University of Tehran, Iran

² Assistant Professor, Earth Physics Department, Institute of Geophysics, University of Tehran, Iran

³ Head of the Department of Geotechnics, Building and Housing Research Center of Iran

⁴ Professor of Geophysics, Department of Earth Sciences, Uppsala University, Sweden

⁵ Master Graduate, Institute of Geophysics, University of Tehran, Iran

(Received: 9 May 2009, Accepted: 11 Oct 2011)

Abstract

Due to their inherent sensitivity to resistivity contrast, EM methods have an important role in detection of fault zones. In this paper, we experienced Controlled Source Tensor Magnetotelluric (CSTMT) method to recognize a fault zone in Bam area. An earthquake devastated the town of Bam on 26 December 2003. Surface displacements reveal that over 2 m of slip occurred at depth on a fault that had not previously been identified. This fault, located in south of Bam, is a strike slip fault which extends from the centre of Bam city southwards for about 12 km. Data were collected along a profile with an approximately NW-SE direction and perpendicular to the fault. The frequency range used in this method is in the range of 1-25 kHz. The CSTMT field measurements resolved well the resistivity contrast along the profile and 1D and 2D inversion models agree well with the data. Consequently, CSTMT is proved to be a useful method for detecting such structures, utilizing tensor data produced by two perpendicular magnetic loops together with a four electric sensor array.

Key words: Resistivity, Fault, CSTMT, Bam, Inversion

شناسایی زون گسله جنوب بم با استفاده از روش CSTMT

داوود مقدس^۱، بهروز اسکویی^۲، سعید هاشمی طباطبایی^۳، لاسط پدرسین^۴ و عزیز ناسوتی^۵

^۱ دانش‌آموخته، گروه فیزیک زمین، مؤسسه ژئوفیزیک دانشگاه تهران، ایران

^۲ استادیار، گروه فیزیک زمین، مؤسسه ژئوفیزیک دانشگاه تهران، ایران

^۳ مدیر بخش ژئوتکنیک، مرکز تحقیقات ساختمان و مسکن ایران، تهران، ایران

^۴ استاد ژئوفیزیک، بخش علوم زمین، دانشگاه ایسلا، سوئد

^۵ دانش‌آموخته، گروه فیزیک زمین، مؤسسه ژئوفیزیک دانشگاه تهران، ایران

(دریافت: ۸۸۲/۱۹، پذیرش نهایی: ۹۰۷/۱۹)

چکیده

در سال‌های اخیر، روش‌های الکترومغناطیسی به‌طور گسترده در آشکارسازی و تشخیص ساختار ژئوالکتریکی محدوده گسل‌ها به کار رفته است. در این مقاله از روش رادیومگنتوتلوریک با چشمه کنترل شده (CSTMT) در تشخیص زون گسلی بم استفاده شد. در دی‌ماه ۱۳۸۲ زلزله‌ای به بزرگی ۶/۵ ریشتر، شهر بم را تخریب کرد. در منطقه ذکر شده، جابه‌جایی‌های سطحی نشان می‌دهد که حدود ۲ متر از لغزش عمقی در گسلی رخ داده است که قبلاً مشخص نشده بود. این گسل جدید که ۱۲ کیلومتر از مرکز شهر به طرف جنوب گسترش دارد امتداد لغز است و بیشینه لغزش آن ۲ متر در عمق حدود ۵ کیلومتر است. یک نیم‌رخ CSTMT شامل نوزده نقطه در جهت شرقی-غربی و عمود بر گسل برداشت شد. نتایج حاصل از وارون‌سازی یک‌بعدی و دوبعدی به خوبی با شبه مقاطع ویژه الکتریکی داده‌ها و زمین‌شناسی منطقه تطبیق می‌کند و به خوبی اختلاف مقاومت ویژه الکتریکی موجود در طول نیم‌رخ را مشخص می‌کند.

واژه‌های کلیدی: مقاومت الکتریکی، گسل، رادیومگنتوتلوریک با چشمه کنترل شده، بم، وارون‌سازی

1 INTRODUCTION

Strike-slip faults such as Bam fault, the San Andreas Fault (SAF) and North Anatolian fault have generated some of the most destructive earthquakes for years. Recognition and study of the active faults has always been the important issue in geosciences. A range of geological and geophysical studies have improved our understandings of the faults. Geophysical methods have been proven to be effective techniques for tectonic studies. In particular, electromagnetic (EM) techniques such as Magnetotelluric (MT), Controlled Source Audio Magnetotelluric (CSAMT) and Controlled Source Tensor Magnetotelluric (CSTMT) methods can provide important information about the faults. In recent years, EM methods are widely used for tectonic studies (Bedrosian et al., 2004, Unsworth and Bedrosian, 2004, Unsworth and Xiao, 2006).

Seismic and Electrical resistivity techniques have been increasingly used for fault studies (Thurber et al., 1997, Caputo et al., 2003, Vanneste et al., 2008). Seismic reflection is a highly effective tool for imaging complex structures. However, in certain conditions, seismic data quality can be severely diminished such as overthrust belts where high-velocity rocks are emplaced over a low-velocity layer. This geometry usually corresponds to high electrical resistivity over low resistivity, which is favorable for structural imaging with electromagnetic methods (Unsworth, 2005). Electrical imaging techniques have also been applied in near-surface geophysics giving significant results to solve a wide range of geological problems particularly for tectonic studies. From a technical point of view, an Electrical resistivity survey is carried out using electrode configurations which necessitates spending a lot of time for data acquisition. However, Electromagnetic methods are noninvasive techniques which enable us to have faster survey. Geological structures depending on their type, fluids and porosity, have different responses to the electromagnetic waves. Fault zones have resistivity contrast particularly when clay

minerals, water and other fluids flow through them; therefore they can be recognized easily by electromagnetic methods. In dry areas such as central Iran a fault zone is characterized differently due to the lack of water and conductive material in the fault zone. Basically the fault zones in such areas are more resistive than the host rocks or sediments.

The controlled source audio-frequency magnetotelluric method proposed by Goldstein and Strangway (1975) is based on measuring one set of horizontal electrical and perpendicular magnetic components. After that, many authors for example Sandberg and Hohmann (1982), Bartel and Jacobson (1987), Hughes and Carlson (1987), have studied this method in detail. Hughes and Carlson suggested using two sources at different places so that tensor quantities are measured. In that way, the electromagnetic transfer functions depend on both positions and orientations of the sources. The method called Controlled Source Audio Magnetotelluric due to the usage of the frequencies in audio range. The CSAMT has proven to be a powerful tool for the exploration of shallow electrical conductivity structures. The CSTMT method introduced by Li and Pedersen (1991) is defined as simultaneous measurements of electric and magnetic fields produced by local transmitters with electric dipoles or magnetic loops at the same position and recording of their time variations at the surface of the earth.

In Iran, the application of geophysical methods for study of faults becomes increasingly important because of devastated earthquakes happening almost all over the country. Bam south fault which was the origin of a devastated Earthquake on 26th December 2003 is one of important shaking structures in Iran. A review of what is known of the historical seismicity of the region is given by Berberian (2005). Talebian et al., (2004), Funning et al., (2005) and Jackson et al., (2006) studied this fault using the Envisat advanced synthetic aperture radar imagery.

Surface effects of the 2003 Bam earthquake also studied by Okumura et al., (2004).

In summer 2006, the CSTMT study was carried out to recognize the fault zone in the south of Bam. Data were collected along a profile with an approximately NW-SE direction and perpendicular to the fault. In this paper, We discuss processing, inversion and interpretation of CSTMT data collected along the profile.

2 GEOLOGICAL SETTING

The city of Bam is located southeast of Kerman. The area of the city is about 5400 Hectares having a smooth topography and morphology. The altitude of the city is approximately 1050 meter above sea level. Climatologically the area has dry weather and the total amount of annual rainfall is not considerable especially during the recent years (Hosseini et al., 2004).

A simplified geological map of the area is presented at the fig.1, based on the 1:250,000

geological map prepared by GSI (Geological Survey of Iran). Five different lithologies can be observed in the main geological formations of the area including: recent Quaternary alluvium, late Quaternary sandstones and siltstones, Paleogene sedimentary rocks, Eocene volcanic rocks, and intrusive igneous rocks (Granodiorite). Quaternary fine sands and silts form the alluvium around the Bam town and its vicinity. These sediments are yellow to brown sand and silt, coarse grain brown gravel deposits of flooded plains, coarse grain gravel of alluvial fans and coarse grain deposits of the rivers, respectively. Bam-Baravat fault is the main tectonic feature in the area that overlaid the old Quaternary sediments on younger sedimentary layers at east of Bam. As a result, the old Quaternary sediments formed a hilly morphology that has been cut by some drainage systems and made several deep channels prone to landslide (Hosseini et al., 2004).

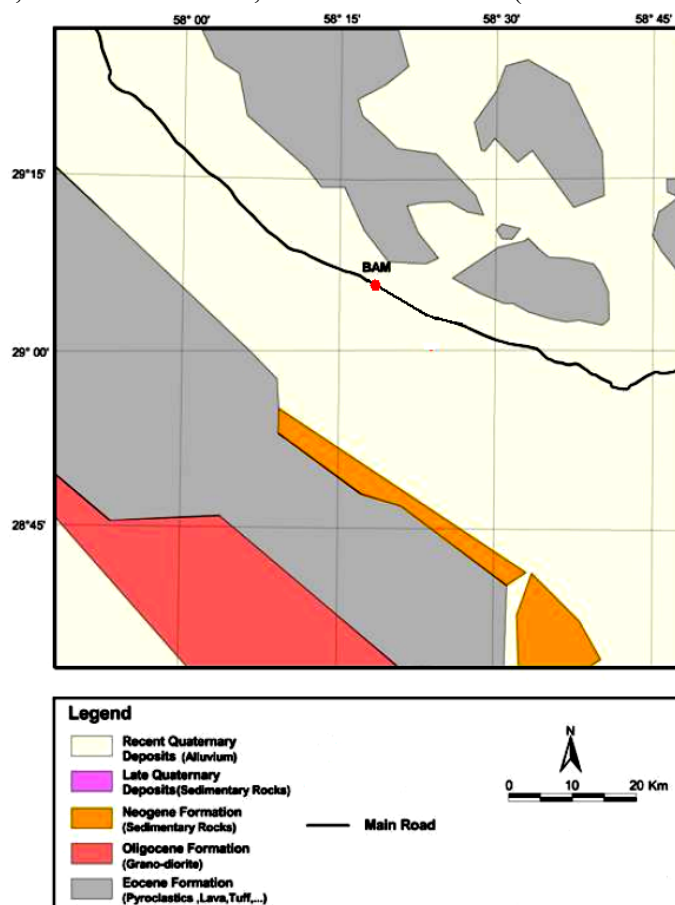


Figure 1. Geological map of Bam area (After Hosseini et al., 2004).

3 BAM'S RECENT EARTHQUAKE

Bam lies within the western of two north-south, strike-slip fault systems located on each side of the Lut desert, which together accommodate the relative motion between central Iran and Afghanistan, part of the Eurasian plate (figure.2). An earthquake devastated the town of Bam on 26 December 2003. Surface displacements reveal that over 2 m of slip occurred at depth on a fault that had not previously been identified (Talebian, et al., 2004). This fault located in south of Bam is a strike slip fault which extends from the centre of Bam southwards for about 12 km. The region is an almost flat, featureless, sloping gently east (figure 3). The absence of

geomorphic indicators, such as topographic features near the fault, or offset drainage channels, can be attributed to several factors. The lack of a vertical component in the fault motion suggest that the topographic signature due to a single earthquake would be of the order of a few centimeters, and therefore many hundreds of earthquake cycles would be needed to build topography. The dominant geomorphic feature in the area south of Bam is an alluvial fan system and the growth of the alluvial fans in the area is likely to be both more rapid and of larger amplitude, than the growth of topography due to motion on the main fault (Funning, et al., 2005).

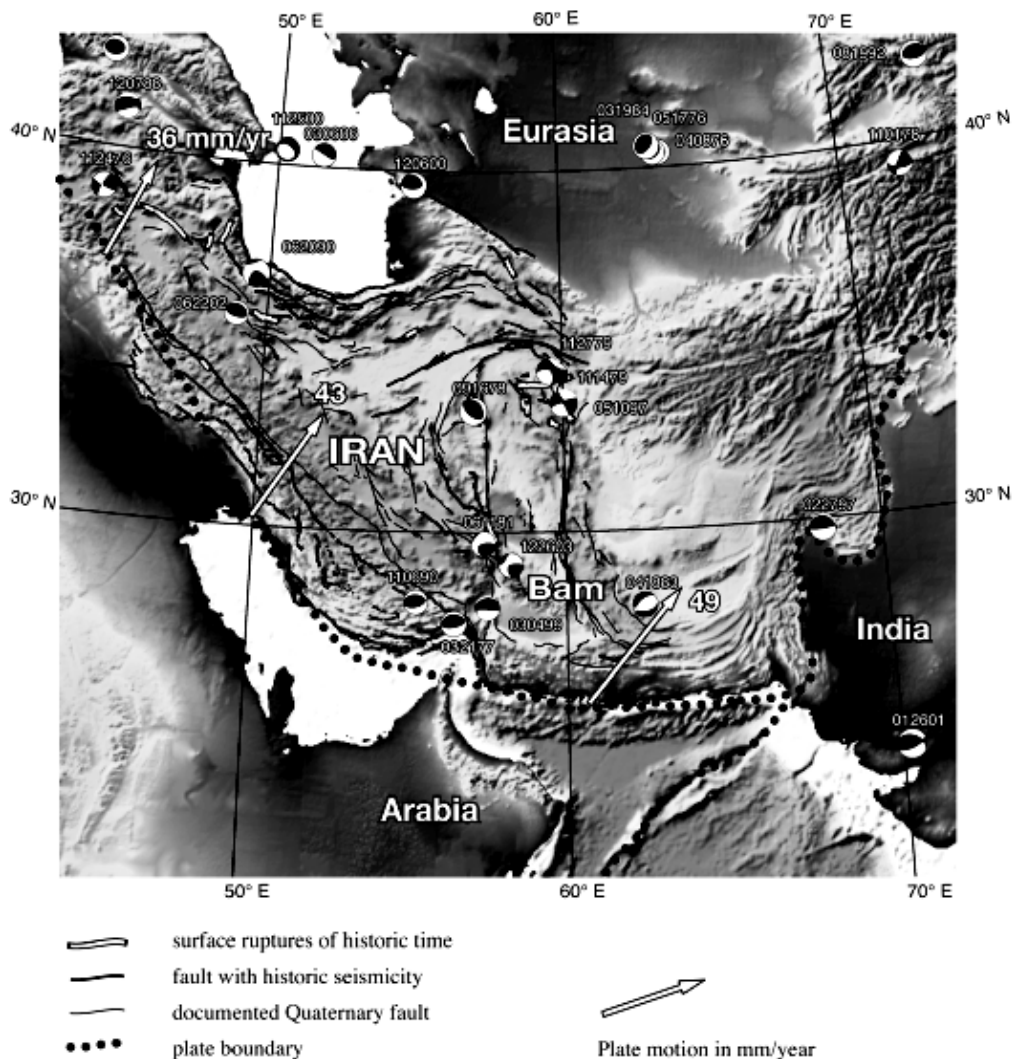


Figure 2. Active tectonics and recent large earthquakes in Iran and adjacent areas (After Okumura et al., 2004).

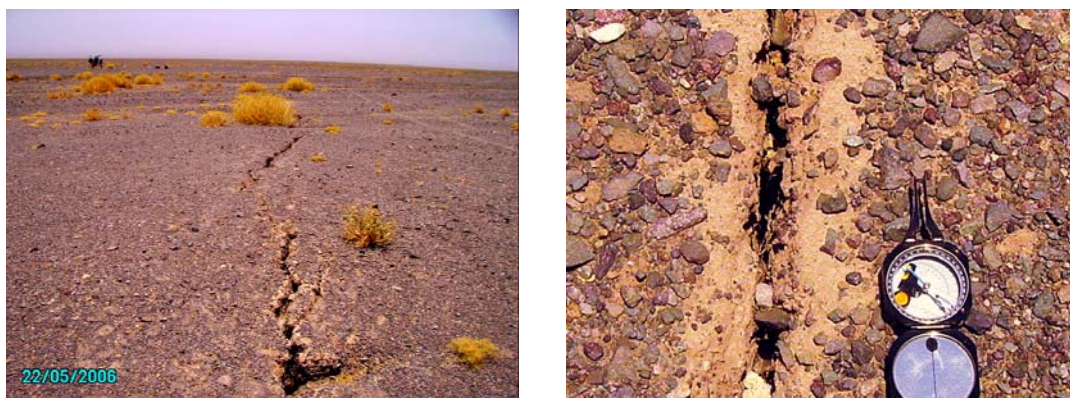


Figure 3. The fault in south of bam is a strike slip fault in a region which is flat and featureless.

4 CSTMT METHOD

The transfer functions of CSTMT data contain information from both parallel and perpendicular to the principal horizontal axes of anisotropy, so that this method is capable of detecting azimuthal anisotropy. In the quasi-static approximation, displacement currents are neglected, and for frequencies less than 250 kHz, this is usually a good approximation (Pedersen, et al., 2005).

Goldstein and Strangway (1975), in their classical paper on CSMT measurements, showed that for a homogeneous half-space, plane-wave conditions prevail if the distance between source and receiver is at least 3–5 times the depth of exploration. But Wannamaker (1997) noted that conductive sediments over resistive basement seriously reduce the depth of exploration within the plane-wave regime to about $1/20^{\text{th}}$ of transmitter-receiver distance.

The frequency band from 1–25 kHz was covered by a double-dipole transmitter consisting of two mutually perpendicular, horizontal magnetic dipoles (vertical coils) tuned to preselected frequencies uniformly distributed along the logarithmic-frequency axis with approximately two frequencies per octave. Each dipole has a cross-sectional area of 27 m^2 , 5 windings, and maximum current of 20 A, giving a maximum dipole moment of 2700 Am^2 . Good timing accuracy is guaranteed by GPS-controlled crystal clocks on both transmitter and receiver sites. The selection and changing of source frequencies and polarizations is governed completely

from the receiver (Bastani, 2001).

The horizontal electric field components are measured in N-S and W-E directions, using two pairs of steel electrodes. The electrodes are set symmetrically with respect to the central box and the electrode separations are the same in both directions. The three magnetic sensors measured magnetic field components. The two horizontal sensors are oriented parallel to the electric field sensors and the third sensor points vertically downwards. After analogue filtering in the AF box the analogue signals from the five channels are transferred to the central unit for subsequent A/D conversion and processing.

5 CSTMT DATA ACQUISITION AND PROCESSING

The CSTMT survey was carried out in summer 2006 using EnviroMT system from Uppsala University, Sweden. Data were collected along a profile with 19 stations and with an approximately NW-SE direction which was perpendicular to the fault. The distance between stations was varying between 5 and 50 m. We mapped 260m of surface ruptures during field survey. Figure 4 shows the location of fault zone and our CSTMT profile. The transmitter was situated 200m away from station number 7 which provided plane-wave conditions.

The time-series were processed to yield estimates of apparent resistivity and phase in the frequency band 1-25 kHz using the method of Li and Pedersen (1991). In this

technique a unique transfer function can be found at the selected transmitter frequencies. This is because the transmitter consists of two independent horizontal dipole coils. According to data pseudo-sections illustrated in Fig.5 phase and apparent resistivity in both xy and yx directions have no agreement.

Consequently, a 2D structure which justifies the use of a 2D modeling must be considered. This sections show two distinct zones: (1) A high resistivity zone (500-1000 ohm.m) around station number 6. (2) A low resistivity zone (10 ohm.m) around station 16.

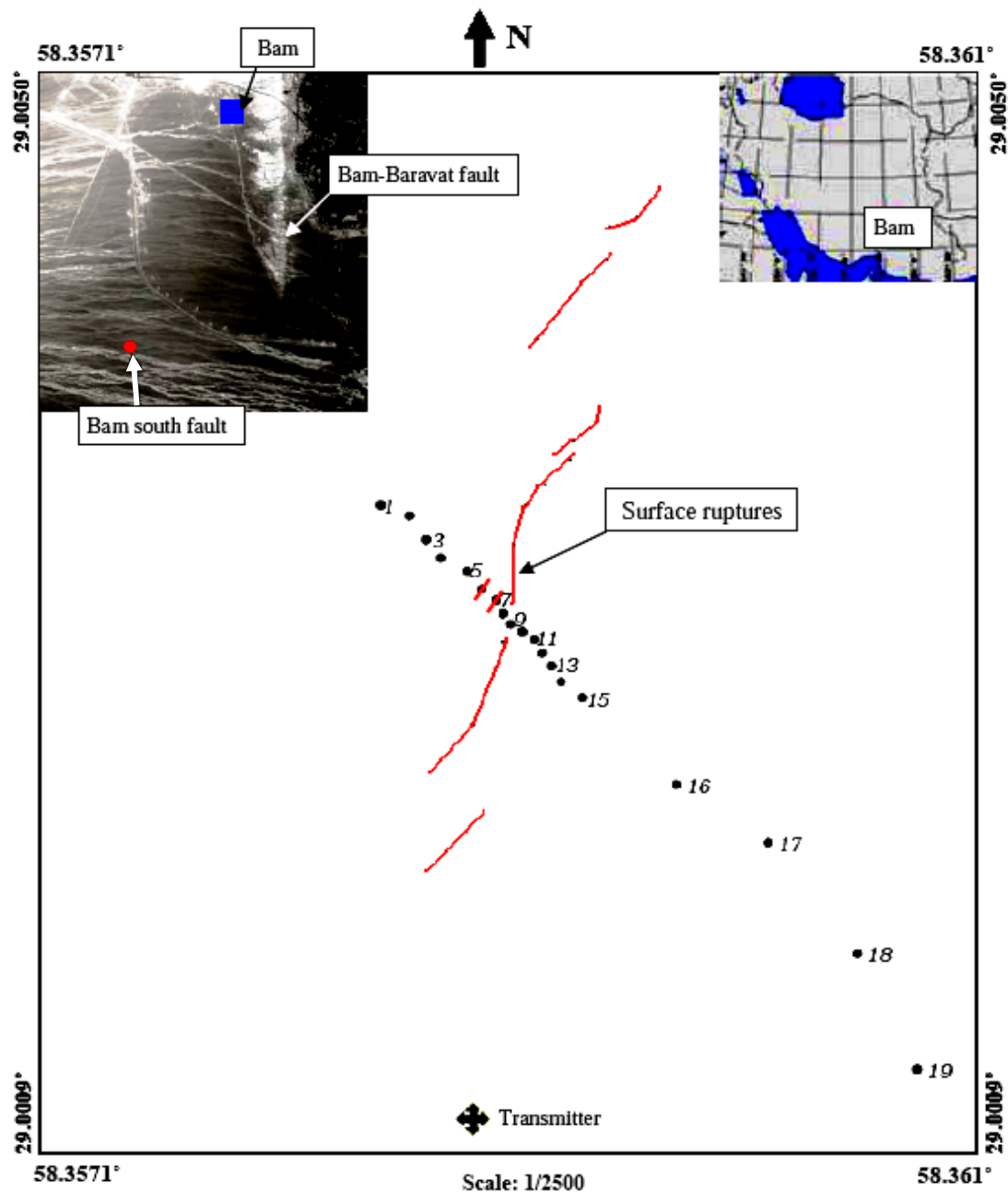


Figure 4. The location of the field site in south of Bam: The CSTMT stations and fault locations are shown respectively by black circles and red lines. Blue and red squares in satellite map respectively illustrate the location of Bam and survey area. To provide plane-wave conditions, the transmitter was situated 200m to station number 7.

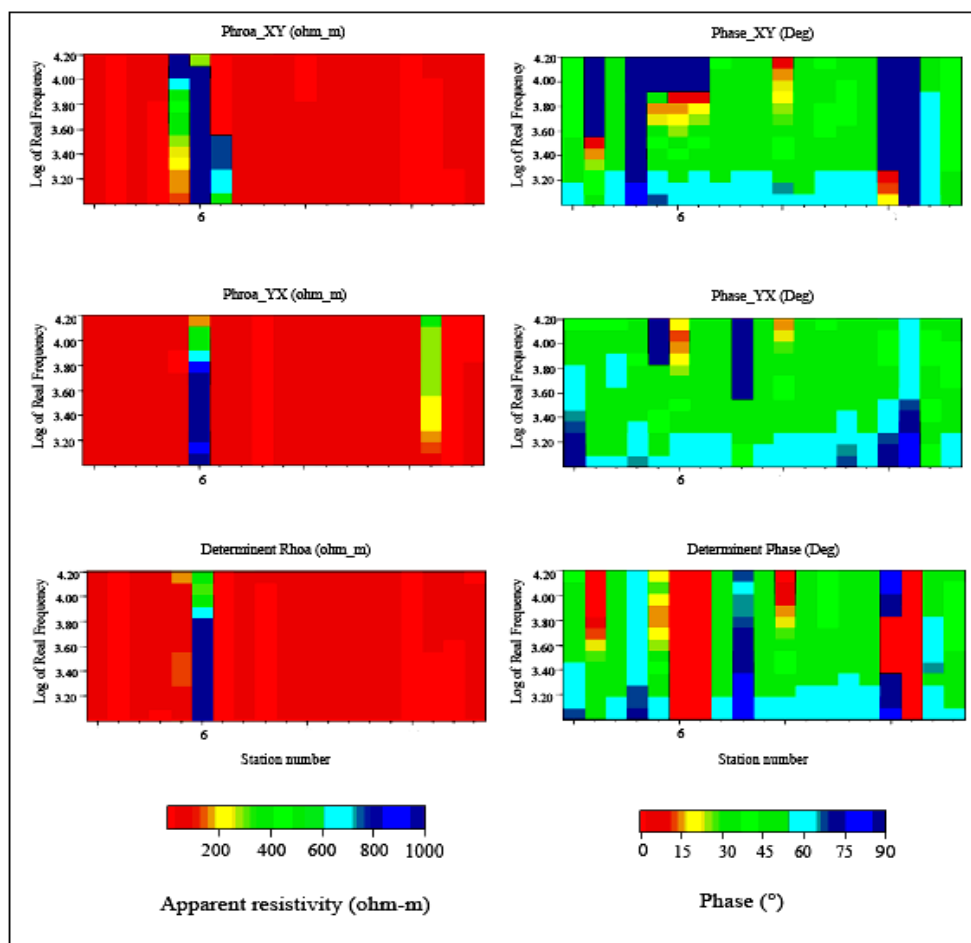


Figure 5. Apparent resistivity and phase.

6 1D MODELING

To interpret the CSTMT data, the next step is converting the data into a model of subsurface resistivity as a function of true depth. This procedure is called inversion. The inversion code presented by Pedersen (2004) was used to obtain 1D model. Input data are apparent resistivities and phases. This algorithm provides a more automatic approach than the standard Occam procedure, which is of particular importance when very large data sets are treated. We assumed 0.05 error floor on the impedance elements.

Having established the reliability of the inversion models, it is important to consider the implication for the fault zone. Fig.6 illustrates the final model of 1D inversion. A resistivity contrast is clearly seen around station numbers 7, 8 and 9. A high resistivity zone in the middle of profile at location of

stations 7, 8 and 9 is recognized compared with the rest of the profile.

7 2D MODELING

As the fault zone has a two dimensional structure, it necessitates to perform 2-D inversion. We performed 2D inversions with the REBOCC code (Siripunvaraporn and Egbert, 2000), which is based on the quasi-static assumption and therefore is an efficient method for the inversion of electromagnetic data. We assumed 0.05 error floor on the impedance elements. This algorithm is also faster than Occam inversion. Fig.7 shows the observed data, model responses and residuals. Because we are searching for minimum norm models, the inversion can be divided into two stages: Phase I for reducing the misfit to the desired level. Phase II is necessary in order to wipe out the spurious

features occurring while the program tries to reduce the misfit (Oskooi, 2004). The final 2D model is shown in figure8. This model clearly illustrates two distinct zones: (1) A high resistivity zone (500-1000 ohm.m) around stations numbers 6 and 7. (2) A low

resistivity zone (10 ohm.m) around station 16. CSTMT results show lateral and vertical variations of resistivities around Bum's south fault which is hidden below the shallow alluvial layers at the location of the city.

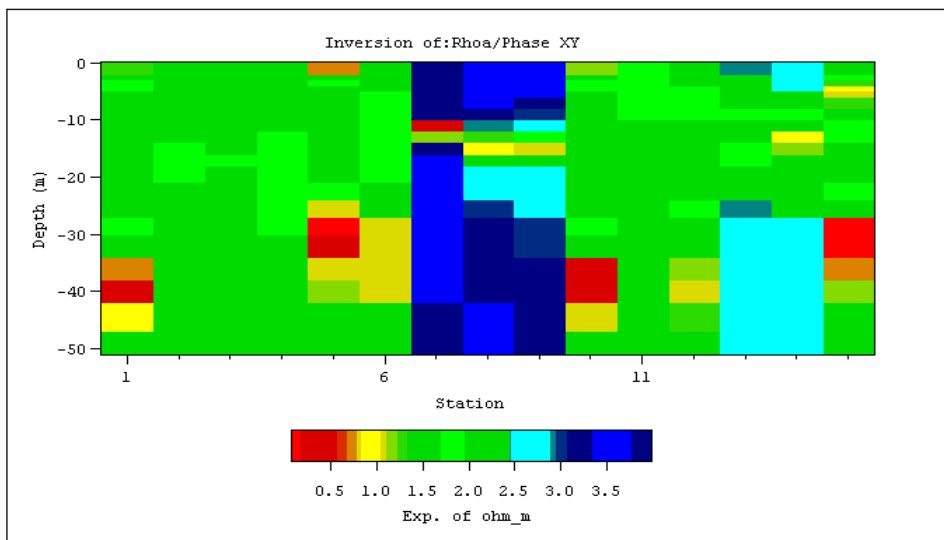


Figure 6. 1D inversion of phase and resistivity data in xy direction along the profile.

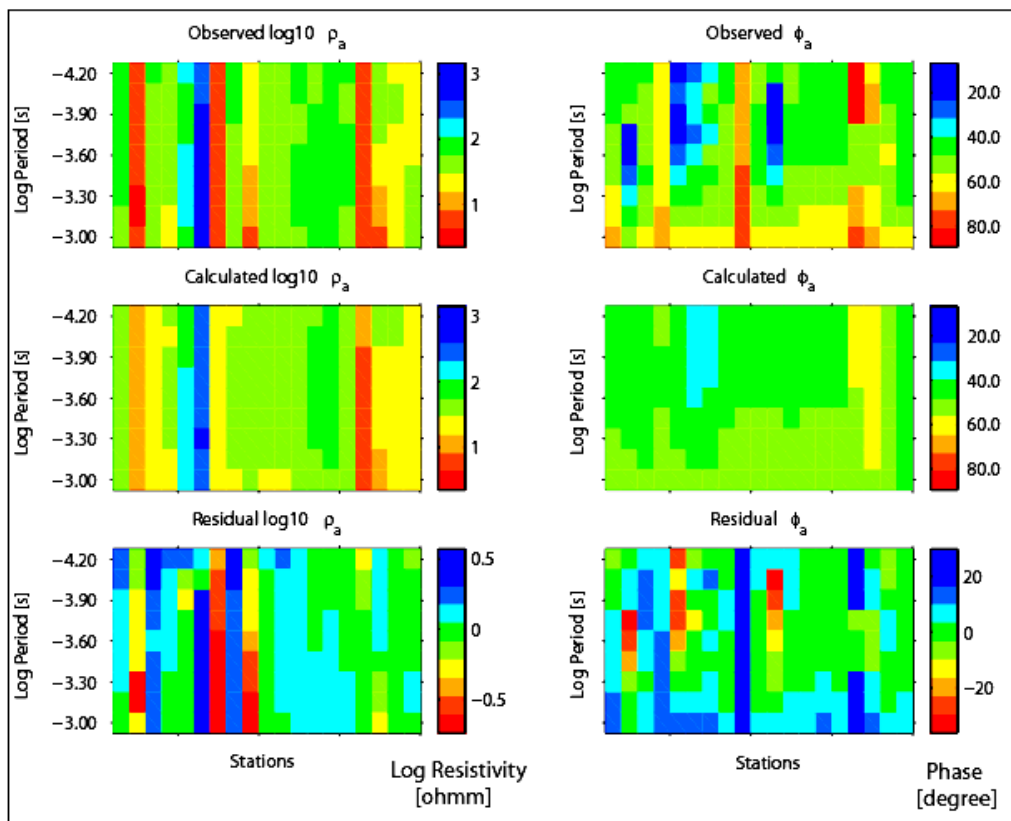


Figure 7. Observed data, model responses and residual.

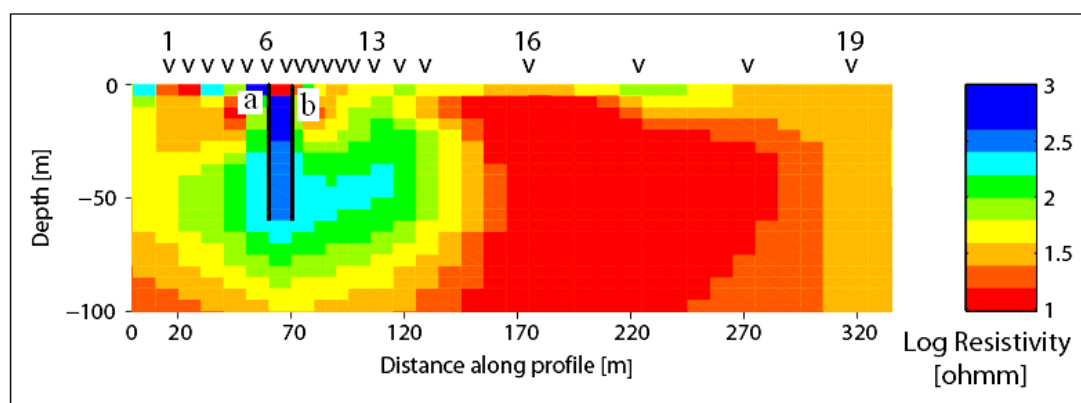


Figure 8. Final 2D model derived from REBOCC inversion: black lines show the trace of the faults in station 6 and 7.

8 DISCUSSION AND CONCLUSIONS

The CSTMT technique is a powerful tool for the recognition of faults and the case study shown in this paper proved the efficiency of this method. Like any geophysical method, CSTMT requires a contrast in material properties to image structures and in the study area the resistivity contrasts occurred in the Quaternary sediments due to a fault zone were detected by this technique. The great advantage of CSTMT lies in the fact that it uses tensor data which provide information from both perpendicular and parallel to strike. Furthermore, local transmitter is employed to overcome the noise problems in this method. Data pseudo-sections show a high resistivity zone (500-1000 ohm.m) at station 6 and a low resistivity zone (10 ohm.m) at station 16. A resistivity contrast is clearly seen at station numbers 7, 8 and 9 in 1D model. 2D model clearly illustrate a high resistivity zone (500-1000 ohm.m) at station numbers 6 and 7 and a low resistivity zone (10 ohm.m) around station 16. The fault zone is located at stations number 6 and 7 (a and b in figure 8). The 1D and 2D inversion of CSTMT data gives the models that agree well with regional geology and data. As the fault zone is a 2D structure, 2D modeling provides more reliable results compared with 1D modeling with respect to the depth and resistivity. High resistivity in fault zone around station 6 and 7 is because of the dry nature of the area of study; so that, ruptures and pores lack water and conductive materials like fine minerals and clay. The

application of this method in regions with high amount of rainfall such as northern Europe leads to reverse results; so that, fault zones illustrate low resistivity compared with their surroundings which is due to the existence of water and clay in ruptures and pores.

ACKNOWLEDGEMENT

We would also appreciate the Building and Housing Research Center of Iran for supporting us in the field logistically and for the accommodation. The EnviroMt system from Uppsala University was used for the measurement which is acknowledged. The 2006 field work was made possible by the hard work and endurance of Mozafar Ghahremani, Majid Zeinali, Abbas Fanaei, Javad asadi Fallah in some challenging field conditions. The research council of the University of Tehran for financial support is acknowledged.

REFERENCES

- Bartel, L. C. and Jacobson, R. D., 1987, Results of a controlled source audiofrequency magnetotelluric survey at the Puhimau thermal area, Kilauea Volcano, Hawaii, *Geophysics*, **52**, 665-677.
- Bastani, M., 2001, A new controlled source radio magnetotelluric system, PhD thesis, Uppsala University, ISBN, 91-554-5051-2.
- Bedrosian, P. A., Unsworth, M. J., Egbert, G. D. and Thurber, C. H., 2004, *Geophysical*

- images of the creeping segment of the San Andreas fault: implications for the role of crustal fluids in the earthquake process, *Tectonophysics*, **385**, 137-158.
- Berberian, M., 2005, The 2003 Bam urban earthquake: a predictable seismotectonic pattern along the western margin of the rigid Lut block, southeast Iran, *Earthquake Spectra*, **21**, S35–S99.
- Caputo, R., Piscitelli, S., Oliveto, A., Rizzo, E. and Lapenna, V., 2003, The use of electrical resistivity tomographies in active tectonics: examples from the Tyrnavos Basin, Greece, *J. geodynamics*, **36**, 19-35.
- Funning, Gareth. J., Parsons, Barry., Wright, Tim. J., 2005, Surface displacements and source parameters of the 2003 Bam (Iran) earthquake from Envisat advanced synthetic aperture radar imagery, *Journal of Geophysical Research*, **110**, B09406, doi: 10.1029/JB003338.
- Goldstein, M. A. and Strangway, D. W., 1975, Audio-frequency magnetotellurics with a grounded electric dipole source, *Geophysics*, **40**, 669-483.
- Hughes, L. J. and Carlson, N. R., 1987, Structure mapping at Trap Spring Oilfield, Nevada, using controlled-source magnetotellurics: *First Break*, **5**, 403-418.
- Hosseini, K. A., Mahdaviifar, M. R., Bakhshayesh, M. K., Rakhshandeh, M., 2004, Engineering geology and geotechnical aspects of Bam Earthquake, primary report. Website: http://www.emsc-sem.org/Doc/BAM_IRAN/bam_report_english_geo%5B1%5D.html.
- Jackson, J., Bouchon, M., Fielding, E., Funning, G., Ghorashi, M., Hatzfeld, D., Nazari, H., Parsons, B., Priestly, B., Talebian, M., Tatar, M., Walker, R. and Wright, T., 2006, Seismotectonic, rupture process, and earthquake-hazard aspects of the 2003 December 26 Bam, Iran, earthquake, *Geophysics. J. Int.*, doi:10.1111/j.1365-246X.03056.x.
- Li, Xiaobo., Pedersen, Laust. B., 1991, Controlled Source Tensor Magnetotellurics, *Geophysics*, **56**, 1456-1461.
- Okumura, K., Kondo, H., Azuma, T., Echigo, T. and Hessami, K., 2004, Surface effects of the December 26th, 2003 Bam earthquake along the Bam fault in southeastern Iran: *Bull. Earthq. Res. Inst. Univ. Tokyo*, **79**, 29-36.
- Oskooi, B., 2004, A broad view on the interpretation of Electromagnetic data (VLF, RMT, MT, CSTMT). Comprehensive summaries of Uppsala Dissertation: ISBN: 91-554-5925-0.
- Pedersen, L. B., 2004, Determination of the regularization level of truncated singular-value decomposition inversion: The case of 1D inversion of MT data, *Geophysical prospecting*, **52**, 261-270.
- Pedersen, L. B., Bastani, M., Dynesius, D., 2005, Ground water exploration using combined controlled source and radiomagnetotelluric techniques, *Geophysics*, **70**, G8-G15.
- Sandberg, S. K. and Hohmann, G. W., 1982, Controlled source audiomagnetotellurics in geothermal exploration: *Geophysics*, **47**, 100-116.
- Siripunvaraporn, W. and Egbert, G., 2000, An efficient data-subspace inversion method for 2-D magnetotelluric data, *Geophysics*, **65**, 791–803.
- Talebian, M., Fielding, Eric. J., Funning, Gareth. J., Ghorashi, Mnoucher., Jackson, James., Nazari, Hamid., Parsones, Barry., Priestly, Keith., Rosen, Paul. A., Walker, Richard., Wright, Tim. J., 2004, The 2003 Bam (Iran) earthquake, Rupture of a blind strike-slip fault: *Geophysical Research Letters*, **31**, L11611, doi: 1029/GL020058.
- Thurber, C., Roecker, S., Ellsworth, W., Chen, Y., Lutter, W. and Sessions, R., 1997, Two-dimensional seismic image of the San Andreas fault in the Northern Gabilan Range, central California, evidence for fluids in the fault zone, *Geophys. Res. Lett.* **24**, 1591–1594.
- Unsworth, M. J. and Bedrosian, P. A., 2004, Electrical resistivity structure at the SAFOD site from magnetotelluric exploration, *Geophysical research letters*, **31**, L12S05, doi: 10.1029/GL019405.

- Unsworth, M. J., 2005, New developments in conventional hydrocarbon exploration with electromagnetic methods, Canadian Society of Exploration Geophysicists Recorder, 34-38.
- Unsworth, M. J. and Xiao, W., 2006, Structural imaging in the Rocky Mountain Foothills (Alberta) using magnetotelluric exploration, *Geohorizons*, **90**, 321-333.
- Vanneste, K., Verbeeck, K. and Petermans, T., 2008, Pseudo-3D imaging of a low-slip-rate, active normal fault using shallow geophysical methods, The Geleen fault in the Belgian Maas River valley, *Geophysics*, **73**, B1-B9.
- Wannamaker, Philip. E., 1997, Tensor CSAMT survey over the Sulphur Springs thermal area, Valles Caldera, New Mexico, U.S.A., Part II: Implications for CSAMT methodology, *Geophysics*, **62**, 466-476.

Appendix 1

Theory of CSTMT

The Maxwell's equations express that for any plane-wave components of the incident electromagnetic field at frequency ω we can write:

$$\begin{bmatrix} E_x \\ E_y \\ H_z \end{bmatrix} = \begin{bmatrix} Z_{xx} & Z_{xy} \\ Z_{yx} & Z_{yy} \\ A & B \end{bmatrix} \begin{bmatrix} H_x \\ H_y \end{bmatrix} \quad (1)$$

where E and H represent respectively the electric and magnetic fields at the surface of the earth. The tensor,

$$Z = \begin{bmatrix} Z_{xx} & Z_{xy} \\ Z_{yx} & Z_{yy} \end{bmatrix} \quad (2)$$

is called the impedance tensor. A and B are magnetic transfer functions and the vector $T = (A, B)^T$ is called the tipper vector. Z and T are functions not only of frequency and wave number, but also vary with position on the surface of the earth. Apparent resistivity and phase are acquired by the following equations:

$$\rho_a = \frac{1}{\mu_0 \omega} \left| \frac{E_x}{H_y} \right|^2 \quad (3)$$

$$\varphi = \tan^{-1} \left[\frac{\text{Im} \left(\frac{E_x}{H_y} \right)}{\text{Re} \left(\frac{E_x}{H_y} \right)} \right] \quad (4)$$

which μ_0 is permeability of free space (Vozoff, 1991). The electromagnetic signals penetrate into the earth to a depth which is termed "skin depth" (δ), that is defined as:

$$\delta \approx 503 \sqrt{\frac{\rho}{f}} \quad (5)$$

which ρ is the resistivity in ohm.m, f frequency in Hz and δ in m. It can be seen that measuring resistivity at greater depths requires lower frequencies. A phase angle is the phase shift between E_x and H_y at a given frequency. If the apparent resistivity increases with decreasing frequency, the phase will be less than 45° . Similarly, a decrease in apparent resistivity will correspond to a phase angle greater than 45° . The phase is generally more sensitive than apparent resistivity to the changes in subsurface resistivity as a function of depth (Vozoff, 1991).

The determinant of impedance tensor which is also called the effective impedance is defined as:

$$Z_{eff} = \left| Z_{xx} Z_{yy} - Z_{xy} Z_{yx} \right|^{1/2} \quad (6)$$

(Berdichevsky, 2001). The advantage of using determinant data is that they provide a useful average for all current directions. Besides, no mode identifications (TE mode: current parallel to

strike or TM mode: current perpendicular to strike) are required, statistic shift corrections are not made and the dimensionality of the data is not considered (Oskooi, 2004).

To estimate the impedance tensor elements in CSTMT method the approach used by Li and Pedersen (1991) is employed. As an example, Z_{xy} and Z_{yx} are given by

$$Z_{xy} = \frac{H_x^x E_x^y - H_x^y E_x^x}{H_x^x H_y^y - H_x^y H_y^x} \quad (7)$$

$$Z_{yx} = \frac{H_y^x E_y^y - H_y^y E_y^x}{H_x^y H_y^x - H_x^x H_y^y} \quad (8)$$

which superscripts x and y represents the dipole source orientation and the subscripts show the x or y components of the measured field.